Use of Subtraction Ictal SPECT Co-Registered to MRI for Optimizing the Localization of Seizure Foci in Children

Pierre Véra, Anna Kaminska, Cécile Cieuta, Andreas Hollo, Jean Louis Stiévenart, Isabelle Gardin, Dorothé Ville, Jean François Mangin, Perrine Plouin, Olivier Dulac and Catherine Chiron

CEA, Service Hospitalier Frederic Joliot, DSV/DRM, Orsay; Department of Nuclear Medicine, Rouen University Hospital and Henri Becquerel Center, Rouen; Department of Neuropediatrics, Saint Vincent de Paul Hospital and INSERM U29, Paris; and Department of Nuclear Medicine, Beaujon University Hospital, Clichy, France

Ictal SPECT studies are increasingly used to localize seizure foci in children with refractory epilepsy, but few studies have reported on ictal-interictal subtraction images co-registered to MRI at this age. **Methods:** Twenty-seven children with partial epilepsy (aged 3 mo–18 y) underwent ictal ethyl cysteinate dimer (ECD) SPECT (20 mCi/1.73 m^2) combined with video-electroencephalography (EEG) and interictal ECD SPECT followed 2 d later by three-dimensional MRI. Ictal-interictal and interictal-ictal subtraction images were computed by registering and normalizing the ictal to the interictal SPECT scans for each child. The ictal, interictal SPECT and subtraction images were registered to each child's MRI. Difference images (ictal-interictal) were then superimposed on MRI for anatomic localization of the perfusion changes. Intra- and interobserver reproducibility and "facility of interpretation" of overlay images were compared with standard analysis of the non-coregistered ictal and interictal scans. **Results:** Overlay images allowed the detection of at least one hyperperfused focus in 93% of the children, compared with 74% using ictal and interictal scans separately. Seizure onset was suspected clinically, on EEG or on MRI in 20 children. Overlay images were concordant (n = 11) or larger (n = 7) than the suspected focus in 18 of 20 (90%), whereas these images failed to show any abnormality in 1 child and were discordant with MRI in another patient. In the remaining 7, images showed cortical localization in 6 patients. Among the 5 patients who underwent electrocorticography, overlay images were concordant in 3, larger in 1 and absent in 1. The intra- and interobserver reproducibility and facility of interpretation were significantly higher using overlay images than standard analysis, even when ictal and interictal SPECT were co-registered. **Conclusion:** The co-registration of ictal-interictal subtraction SPECT images to MRI seems to be a helpful technique in localizing the onset of seizure and guiding the intracranial recording in childhood epilepsy. Moreover, this method improves sensitivity, enhances intra- and interobserver reproducibility and makes interpretation easier.

Key Words: epilepsy; children; SPECT; ^{99m}Tc-ethyl cysteinate dimer; image fusion; co-registration

J Nucl Med 1999; 40:786–792

Children with refractory partial seizures increasingly are referred for epilepsy surgery. Postsurgical outcome is linked closely to accurate localization of the epileptogenic focus, which is especially difficult in infantile epilepsy. Precisely localizing the epileptogenic focus and delineating the epileptogenic region of the cortex to be removed requires invasive electroencephalography (EEG) recordings (*1*). Video-EEG provides a first-line noninvasive approach, but it can fail to localize the site of seizure onset or even be misleading. MRI often discloses cerebral lesions, but their role in causing epilepsy remains to be demonstrated (*2*).

Noninvasive functional neuroimaging techniques using PET and SPECT have proven helpful in localizing epileptic foci in adults, with ictal SPECT providing the highest sensitivity (*3,4*). The first reports of ictal SPECT in children are promising (*5–10*) but still too few for comparison with other methods (*4*).

SPECT images usually demonstrate hypoperfusion interictally and hyperperfusion ictally, and they are traditionally analyzed visually. Localization sensitivity is claimed to be better than 90% in temporal lobe seizures but much lower in extratemporal epilepsies, the most frequent type in children (*6,7*). Several researchers have pointed out the importance of combining visual analysis of both ictal and interictal imaging to improve sensitivity (*4,5*). The first attempts to perform subtraction from ictal to interictal SPECT scans increased the localizing value in temporal and extratemporal lobe seizures (*11,12*).

The aim of this study was to evaluate the usefulness of this type of procedure in children, especially those younger than 4 y old, using ^{99m}Tc-ethyl cysteinate dimer (ECD) SPECT and ictal-interictal scans co-registered to MRI.

MATERIALS AND METHODS

Patients

A total of 44 children were selected for ictal SPECT. Of these, 17 were excluded because ECD could not be injected during seizures (n = 11), injection was postictal (n = 1) or interictal SPECT (n =

Received May 20, 1998; revision accepted Sep. 18, 1998.

For correspondence or reprints contact: Pierre Véra, MD, PhD, Henri Becquerel Center, Department of Nuclear Medicine, 1 rue d'Amiens, 76000 Rouen, France.

2) or MRI (n = 3) were not performed. The remaining 27 children, aged 3 mo to 18 y (mean age 6.5 y), were included in the study (Table 1). Twenty-six had pharmaco-resistant partial epilepsy. MRI disclosed cerebral lesions in 17 of these 26 patients. No lesion was detectable in the others. One remaining child disclosed facial hemispasms as the result of a cerebellar hamartoma. Determination of seizure focus was performed independently by two clinical experts using video-EEG and MRI in all children and using electrocorticography (EcoG) in 5 children. Differences were resolved by consensus. Twelve patients have now undergone surgery, but their outcome could not be used as a final localization of the seizure site in this series, because follow-up was too short.

Protocol

All children underwent ictal and interictal SPECT after intravenous injections of 740 MBq (20 mCi) ^{99m}Tc-ECD for 1.73 m^2 while maintained on their usual antiepileptic drugs. For ictal studies, children received injections during video-EEG–documented seizures at a mean injection time after seizure onset of 15 s (5–30 s). Seizures ranged from 8 to 120 s, and there was no postictal injection in this series, confirmed by video-EEG. Interictal SPECT and MRI were performed 48 h later. Patients younger than 6 y and those who were not cooperative were sedated with intrarectal pentobarbital (5 mg/kg) just before the SPECT scan.

SPECT Scans

Ictal and interictal SPECT acquisitions were performed 1 h after the ^{99m}Tc-ECD injection, using a double-head rotating gamma camera (DST; SMVi, Buc, France) equipped with ultra-high-resolution fanbeam collimators. For each ^{99m}Tc-ECD SPECT scan, 64 angular views of 60 s each were obtained through a 360° circular orbit (32 angular views per head). The SPECT images were reconstructed from projection data using the filtered backprojection algorithm with a 0.5-cutoff frequency Hann filter and a software zoom of 2 (matrix 128 × 128, 16 bits, 128 slices, voxel size 1.7 mm). No attenuation correction was performed. The acquisition and reconstruction parameters used have proven to be the best adapted for standard brain SPECT studies in clinical practice in our department (*13*). Reconstructed brain slices were reoriented according to the bicommissural line (AC-PC) with validated software (*14*). Three sets of axial, sagittal and coronal slices, covering the whole brain, were obtained for ictal and interictal perfusion scans.

TABLE 1
Clinical, Electroencephalography, Electrocorticography, MRI and SPECT Findings*

Patient no.	Age	Sex	Diagnosis	Clinical localization: Clinical seizure	Clinical localization: Ictal EEG	MRI	EcoG	SPECT localization: Overlay images
1	13 y	M	Cortical dysplasia	RFrT	RFrT	RFrT		RFrT
2	10 mo	F	Tuberous sclerosis	LO	LO	LO	LO	LO
3	3 mo	M	Hemimegaloencephaly	RC	RC	R hemispheric		RC
4	18 mo	M	Cortical dysplasia	LFr	LF	LFr		LFr
5	4 y	M	Cortical dysplasia	RFr	RF	RFr		RFr
6	12 y	F	Tuberous sclerosis	RP	†	RP		Bi Fr + RP
7	7 y	M	Tuberous sclerosis	RFr	†	RFr	RFr	Bi Fr + LT
8	17 y	M	Cortical dysplasia	RFrT	RF	RT		RFrT
9	3 y	F	Tuberous sclerosis	RFr	†	RFr		Bi Fr
10	18 y	F	Hypothalamic hamartoma	Hypothalamic	†	Hypothalamic		Hypothalamic
11	5 y	F	Cortical dysplasia	†	†	RF	RF	†
12	10 y	F	Hemispheric atrophy	RFr	†	R hemispheric		RFrT
13	10 y	F	Cryptogenic	LFr	†	†		LFrT
14	8 y	F	Cryptogenic	†	RT	†	RT	RT
15	4 y	M	Cryptogenic	†	RT	†		RPT
16	1 y	F	Cryptogenic	†	RFrT	†		Bi FrT
17	2 y	M	Cryptogenic	†	LO	†		LO
18	17 y	M	Hypothalamic hamartoma	†	†	Hypothalamic		LO
19	3 y	M	Cerebellar hamartoma	†	†	L cerebellar		L cerebellar
20	4 y	F	Tuberous sclerosis	†	†	LFrTP	L FrTP	LFrTP
21	17 y	M	Encephalitis	LC	RT	†		Bi C
22	4 y	F	Hemispheric lesion	†	†	L hemispheric		LFrP
23	3 y	F	Cryptogenic	†	†	†		Bi Fr
24	2 y	M	Cryptogenic	†	†	†		Bi Fr(L > R)
25	2 y	F	Tuberous sclerosis	†	†	Multiple		RFrT
26	4 y	M	Cryptogenic	†	†	†		†
27	2 y	F	Cryptogenic	†	†	†		Bi Fr

*These images correspond to the highest level of perfusion increase.
†Nonlocalizing.
EEG = electroencephalography; EcoG = electrocorticography; R = right; Fr = frontal; T = temporal; L = left; O = occipital; C = central; P = parietal; Bi = bilateral.

MR Images

MR images were obtained just after the interictal SPECT using a 1.5-T MR imager (Signa; General Electric, Milwaukee, WI). Each subject was positioned so that the MRI axial slices were parallel to the bicommissural line (AC-PC) (*15*), which was verified on a midsagittal image. T1-weighted 1-mm-thick axial slices were obtained throughout the whole brain (repetition time = 400–480 ms, echo time = 12 ms, 256 × 256 matrix, 124 slices, 1.03 mm pixel size).

MRI-SPECT Co-Registration

The procedure is summarized in Figure 1. First, interictal and ictal SPECT and MR images were transferred over the Ethernet network to a Sun SPARC-station II (Sun Microsystems, Mountain View, CA). Second, the interictal and ictal perfusion scans of each child were registered to the child's MR image using a computerized three-dimensional registration program developed and validated in our department (*16*). Briefly, discrete representations of the head surface were extracted automatically from the SPECT and MR images. Then, a shape-independent surface-matching algorithm was used to give a rigid body transformation, which permitted the transfer of information between the two modalities. Optimal transformation was inferred from the minimization of a quadratic generalized distance between the discrete surfaces of the two modalities. Finally, the MR images were co-registered to the SPECT images using a rotation matrix and a translation vector. Third, for each child, extracted MRI boundaries were co-registered to the interictal and ictal perfusion scans to verify the accuracy of co-registration. Fourth, the co-registered ictal and interictal perfusion scans were normalized according to the mean pixel counts in the brain and were subtracted from each other to obtain ictal-interictal images, which were computed (*12*). Fifth, subtraction images were smoothed with a three-dimensional Deriche filter ($\alpha = 1$) (*17*). Finally, 20%, 30% and 40% of the maximum of the smoothed subtraction images were superimposed successively on MR images (overlay images). The complete procedure of SPECT reconstruction, co-registration, subtraction, smoothing and superimposition requires approximately 2 h of operator interactive handling and central processor unit calculation.

Image Analysis

To test the intra- and interobserver reproducibility of images, three sets of images were independently read by two observers and by one of them 2 mo apart. The three sets of images were (a) the ictal and interictal perfusion scans reoriented according to the bicommissural line, representing the standard clinical conditions in our center (set 1); (b) the co-registered ictal and interictal perfusions scans superimposed to the extracted MRI boundaries (set 2); and (c) the subtraction images superimposed on MR images (overlay images) (set 3). For each set, the three thresholds (20%, 30% and 40%) were examined, and the one that disclosed the most perfusion abnormalities (most often 40%) was selected for further analysis. For the three sets of images, side and localization of the perfusion abnormalities were classified as involving one or more of the following regions: frontal (Fr), temporal (T), parietal (P) and occipital (O) lobes, and central region (C), basal ganglia (BG) and cerebellum (Cereb). Discordances were resolved by a third observer. For each set of images, observers quantified the facility of interpretation on a scale ranging from 0 (difficult) to 10 (easy). For the co-registered ictal and interictal perfusion scans superimposed on the extracted MRI boundaries (set 2), observers quantified the quality of co-registration on a scale ranging from 0 (bad) to 10 (good).

Statistics

Mean and SD were used for descriptive statistics. Agreement was used to described concordance of the localization of epileptogenic foci between the different sets of images and to evaluate intra- and interobserver reproducibility. The resulting data from quality of co-registration and facility of interpretation were analyzed by repeated measure analysis of variance. $P \leq 0.05$ was considered significant.

RESULTS

Standard Evaluation: Video-Electroencephalography and MRI Analysis

Localizing the onset of a seizure by clinical ictal semiology was possible in 13 of 27 children (Table 1). On scalp EEG, localizing the side and affected lobe was possible in 11

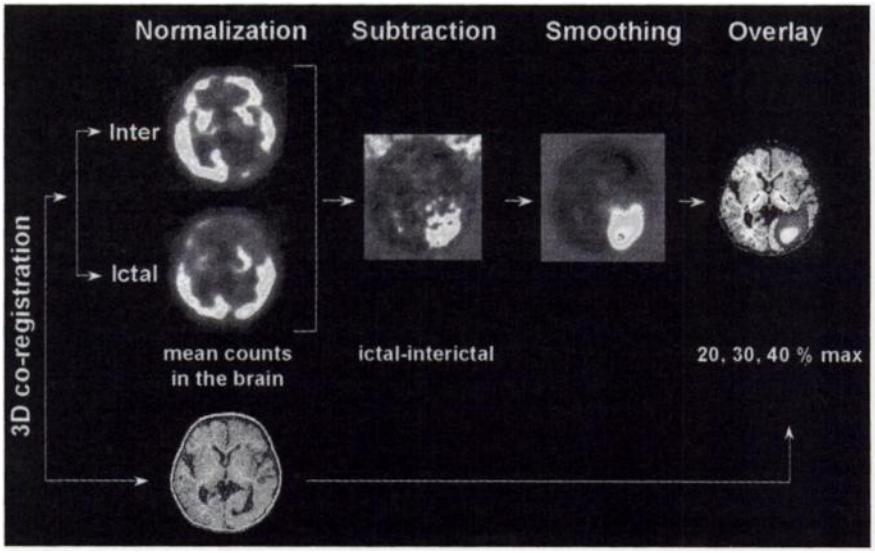

FIGURE 1. Image analysis. Ictal and interictal scans and MRI were co-registered. Co-registered ictal and interictal perfusion scans were normalized according to mean pixel counts in brain. Subtraction images were calculated. Overlay images were smoothed using three-dimensional Deriche filter (a = 1). Then, 20%, 30% and 40% of maximum of smoothed images were superimposed on MR images (overlay images).

of 27 patients. Determining the site of onset of seizures was based on consistent data on the three following features: clinical ictal semiology, EEG and MRI in 5 of 27 patients (patients 1–5; group 1) and on two of these three features in 5 more patients (patients 6–10; group 2). In 10 of 27 patients (patients 11–20; group 3), only one feature was localizing. In the remaining 7 patients (patients 21–27; group 4), it was not possible to localize seizures. Five patients underwent EcoG, which confirmed the site of onset of seizures as previously suspected (patients 2, 7, 11, 14 and 20).

Using SPECT overlay images, 25 of 27 patients exhibited at least one focus of hyperperfusion. Foci were cortical in 23 patients and located only in the hypothalamus or cerebellum in the other 2. More than one cortical focus was observed in 14 of 23 patients. A hyperperfused focus was associated in the cerebellum in 10 patients and the subcortical structures in 6 (Table 2).

Comparison of Overlay Images with Standard Evaluation: Video-Electroencephalography and MRI Findings

For all 5 children in group 1 (patients 1–5), overlay images were concordant with the localization of the focus from the standard evaluation. For group 2, (patients 6–10), overlay images were concordant for 2 of 5 patients (patients 8 and 10), including 1 patient with hypothalamic hamartoma (Fig. 2), and larger (extending to other lobes) than clinical, EEG or MRI findings in 3 others (patients 6, 7 and 9). For group 3 (patients 11–20), overlay images were concordant in 4 of 10 children (patients 14, 17, 19 and 20), larger in 4 (patients 12, 13, 15 and16), discordant in 1 (patient 18) and showed no perfusion abnormalities in 1 (patient 11). Therefore, of the 20 patients for whom the onset of seizure could be localized on the basis of at least one component of standard evaluation, the location given by overlay images was in agreement for 18 (90%). Finally, in group 4 (patients 21–27), for whom localizing the onset of seizures was not possible, overlay images showed an area of hyperperfusion

TABLE 2
Localization of Hyperperfused Foci on SPECT Images

	Interictal and ictal images	Overlay images
Cortical	20/27	23/27
Multiple	14	14
Single	6	9
Cerebellum	1/27	10/27
Homolateral		3
Contralateral	1	4
Bilateral		3
Subcortical	4/27	6/27
Putamen	2*	4
Thalamus	2	2
Hypothalamic		1/27

*Impossible to distinguish from insula.

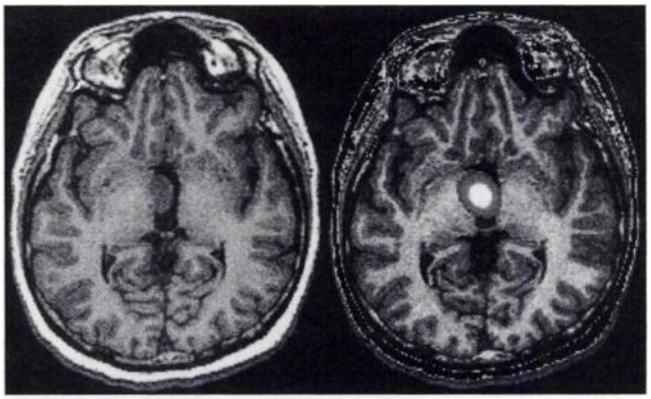

FIGURE 2. Overlay images in 18-y-old woman with hypothalamic hamartoma.

in 6 of 7 children (patients 21–25 and 27) and none in the remaining child (patient 26).

Among the 5 patients who underwent EcoG (patients 2, 7, 11, 14 and 20), overlay images were concordant in 3 (patients 2, 14 and 20), larger in 1 (patient 7) and showed no perfusion abnormalities in 1 (patient 11).

For the entire series, the temporal lobe was involved in 5 patients (patients 1, 8, 14, 15 and 21). In 2 of these (patients 1 and 8), overlay images showed the temporal pattern combining hyperperfusion in temporal, frontal and basal ganglia ipsilaterally and cerebellum contralaterally, as previously reported (*18*) (Fig. 3).

Comparison of Overlay Images to the Classic Ictal-Interictal Scan Analysis

Ictal versus interictal classic analysis (i.e., with no co-registration or normalization) showed cortical abnormalities in 20 of 27 children, compared with 23 of 27 when using overlay images (Table 2). Overlay images were more sensitive in detecting single areas of hyperperfusion in the cortex, cerebellum or basal ganglia, as well as in the hypothalamus. This result was confirmed by the relatively low agreement between non-coregistered ictal and interictal scans (set 1) and overlay images (set 3) (Table 3). Agreement was improved by co-registering images (set 2 versus set 3). Only overlay images were able to separate hyperperfusion in putamen and in insula (Fig. 3).

Observer Analysis

The quality of co-registration was estimated to be 8.4 ± 1 for observer 1 and 7.9 ± 1 for observer 2 (P = NS). The facility of interpretation was estimated to be 4.0 ± 1.6 for ictal-interictal scans (mean of the two observers) (set 1), 5.8 ± 1.6 for co-registered ictal-interictal scans (set 2) and 8.0 ± 1.6 for overlay images (set 3) ($P < 0.0001$) (Fig. 4). Intra- and interobserver agreement were higher for overlay images (set 3) compared with interictal-ictal scans, even when interictal and ictal scans were co-registered (Table 4).

DISCUSSION

This study provides a series of ictal SPECT data in young epileptic infants and demonstrates that the co-registration of

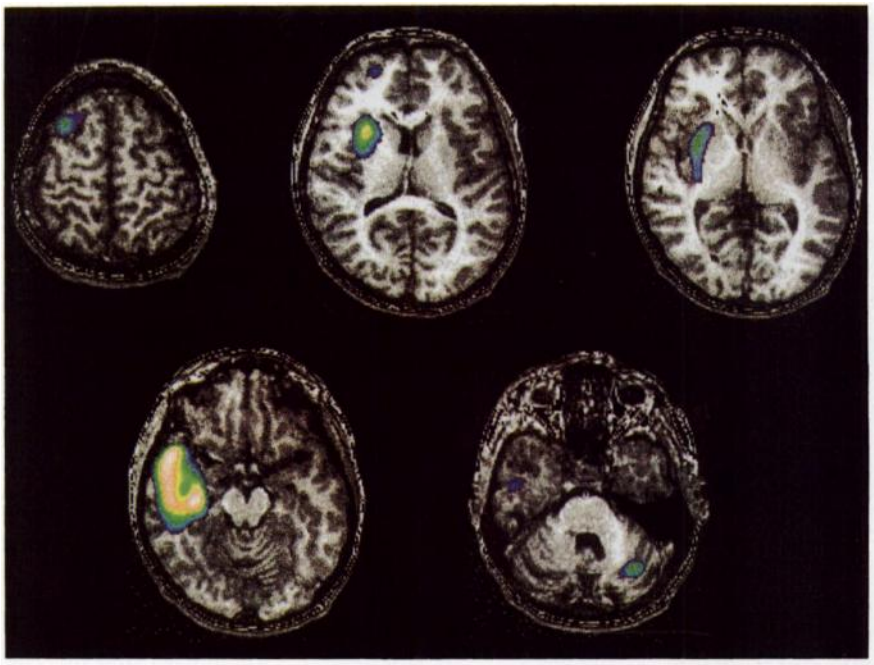

FIGURE 3. Overlay images in 13-y-old boy with temporal dysplasia. Overlay images show temporal pattern with hyperperfusion in homolateral temporal lobe, homolateral putamen, homolateral frontal cortex and contralateral cerebellum. Notice good anatomic localization of hyperperfusion.

ictal, interictal and MR scans is a useful procedure in this population. Ictal-interictal SPECT subtraction images disclose the hyperperfused focus in a location that is in agreement with the epileptogenic focus, based on the other noninvasive methods and intracranial EEG recordings. Overlay images demonstrate higher sensitivity, higher intra- and interobserver agreement and higher facility of interpretation than the standard analysis of the two scans alone. Therefore, such an image processing improves the ability to localize foci in children with intractable partial epilepsy.

Need for Ictal SPECT in Children

Ictal SPECT is proven to be the most sensitive imaging technique to localize noninvasively the epileptogenic focus in temporal lobe epilepsy in adults. Meta-analytic sensitivity rises from 0.44 to 0.97 for interictal to ictal SPECT, in accordance with standard evaluation or surgical outcome (*4*), whereas interictal fluorodeoxyglucose PET or MRI alone reaches a sensitivity of about 0.70 (*3,19*). In extratemporal lobe epilepsies, meta-analysis is still not possible, but sensitivity is about 0.35, although this can be doubled if the tracer is injected early in the course of the seizure (*20–22*). Data are insufficient to draw conclusions regarding the pediatric population with epilepsy (*4*). Moreover, fewer than 10 isolated cases involve children younger than 4 y (*23–25*). Preliminary reports nevertheless revealed a hyperperfused focus consistent with the epileptogenic area in more than 95% of the patients (*5,6,8,9,26,27*) compared with 25%–80% using interictal SPECT.

Noninvasive identification of the epileptogenic focus is of particular importance for children, but is usually more difficult to achieve than in adults. The reasons for this are (a) the clinical semiology of partial seizures is difficult to assess in young children (*28*), and the anatomo-clinical relationships are not as clearly established as in adults; (b) the seizure onset is often apparently generalized or lateralized to a whole hemisphere and cannot contribute to localizing the focus; (c) most epilepsies are extratemporal in origin at this age, resulting in a panel of frontal, rolandic, parietal or

TABLE 3
Agreement on Image Sets Between Two Observers

Agreement	Set 1 vs. set 2	Set 1 vs. set 3	Set 2 vs. set 3
Observer 1	66%	62%	81%
Observer 2	65%	61%	75%

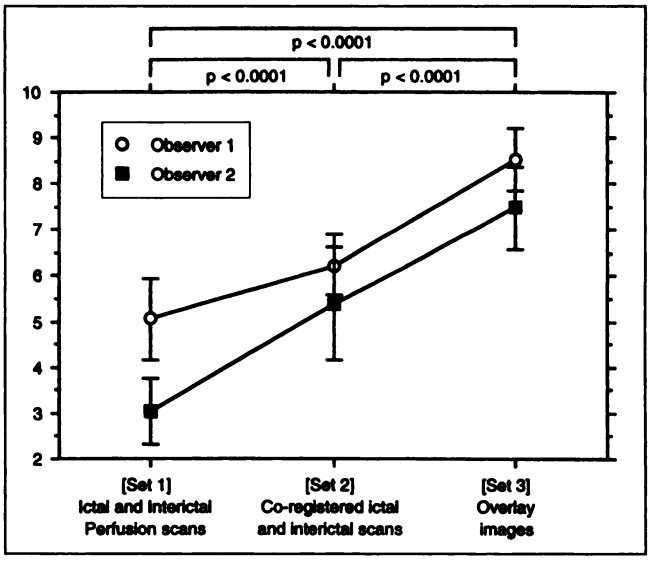

FIGURE 4. Facility of interpretation for different sets of images for two observers.

TABLE 4
Intra- and Interobserver Agreement

Agreement	Interictal and ictal perfusion scans set 1	Co-registered interictal and ictal scans set 2	Overlay images set 3
Intraobserver agreement			
Observer 1 vs. observer 1	70%	78%	83%
Interobserver agreement			
Observer 1 vs. observer 2	71%	74%	85%

occipital foci, which are known to be more difficult to localize than the temporal ones; and (d) a higher proportion (30%) of patients do not exhibit any lesion on MRI. A lesion is a useful guide for localizing the epileptogenic focus, although the epileptogenic zone cannot be superimposed on the lesion, and resecting the latter may fail to cure the epilepsy (*2*).

Need for Subtraction Images

Regarding the localization of focus, visually comparing ictal and interictal cerebral perfusion images is superior to analyzing ictal or interictal ones separately (*5*), and co-registering ictal, interictal and MR images is superior to visually comparing scans (*11*).

Zubal et al. (*12*) showed that the difficulties that arise when SPECT perfusion scans are visually compared result from (a) the lack of normalization of both studies arising from differing brain uptakes of the radiopharmaceutical, even within a single patient; (b) the difficulty of accurately comparing both examinations slice by slice, resulting from differences in patient positioning during the two studies; (c) the lack of quantitative assessment of the difference between the two sets of images; and (d) the poor ability of perfusion scans to demonstrate anatomy (*12*). With our methodology, these four points are solved respectively by (a) normalization of both sets of images; (b) co-registration of ictal and interictal scans; (c) subtraction of both scans; and (d) superimposition of subtraction images to MRI. Moreover, these four steps are objective and observer independent.

Normalization

In this study, normalization is based on mean counts in the brain as previously reported with ^{99m}Tc-hexamethyl propyleneamine oxime (*12*) and ^{99m}Tc-ECD (*11*). Theoretically, other normalization schemes are possible for white matter, cerebellum and brain stem, but these have not been tested.

Co-Registration

Co-registration is performed with a validated method developed in our department (*16*). The error of co-registration with this procedure is 2.14 ± 0.62 mm (mean ± SD) with a maximum difference of 3.18 mm (inferior to 1 pixel, 3.4 × 3.4 mm). The individual quality of co-registration is verified for each child by co-registering ictal and interictal scans with segmented MRI boundaries (set 2) and by agreement by both observers that the quality of co-registration is estimated to be good. Co-registration with this method can be performed successfully, even in young children.

Subtraction

The subtraction images show the localization of the greatest perfusion changes between ictal and interictal scans, but do not show the percent changes between these two conditions. Overlay images are dedicated therefore to localizing rather than quantifying in this series.

Threshold

Two methods have been proposed to quantify subtraction images (*11,12*), but each supposes the same threshold for all patients. In our experience with children and infants, the minimal threshold for detecting at least one subtraction image varied across the whole series. The fact that the threshold may be modified by age and disease has been suggested in a previous functional imaging study in pediatric patients (*29*). We therefore decided to generate images at three different thresholds (20%, 30% and 40%) around the consensus of 30% used in PET activation studies in adults. The threshold showing the most perfusion abnormalities was selected for observer analysis, to detect any ictal change. The remaining two thresholds were used by physicians and neurosurgeons in clinical practice as visual confirmation of this analysis.

Need for Subtraction Scans in Children

This study, which focuses on children and includes 16 of 27 (59%) younger than 4 y, shows that the method of subtraction–co-registration can be applied successfully to such a population. In a preliminary study, we showed that 16 of 17 children exhibited a coherent focus of hyperperfusion (*30*). Overlay processing improved the ability to detect and localize an increased perfusion area from 74% (20/27) to 93% (25/27) of patients in this series, although most have extratemporal epilepsy. Difference images contain significantly more information than can be detected by visually analyzing the reconstructed scans alone, even after co-registration and normalization. Such information is clinically relevant, because the focus of hyperperfusion corresponds to the onset of seizures in 90% (18/20) of patients in whom it could be localized.

Moreover, this type of image processing improves SPECT interpretation by making scans easier to interpret and by increasing the intra- and interobserver agreement compared with ictal and interictal scans alone. This is especially significant for pediatric neurologists, because the age-dependent perfusion changes that result from brain maturation make pediatric images more difficult to read than those of adults.

Significance of Subtraction Images

The significance of multiple foci of hyperperfusion present in some patients is in question. Depending more or less on the threshold selected, foci can be revealed on the

subtraction images. Those with the highest level of perfusion increase have been shown to be the closest to the epileptogenic focus (*12*). Other foci, which may support the propagation of the seizure, are usually detected (*20–22,31*). The multiple foci observed in this study also could be related to seizure discharge, but more extensive intracranial EEG data are needed to confirm this hypothesis in children.

CONCLUSION

This study shows that ictal SPECT procedure and SPECT-MRI co-registration is feasible, even in young children. Perfusion changes seen on overlay images are concordant with clinical, EEG and MRI findings. These images contain more information, provide more precise anatomic localization, are more reproducible and are easier to interpret than standard visual comparison of ictal and interictal scans.

ACKNOWLEDGMENTS

The authors gratefully acknowledge the contribution of Dr. Philippe Kahane for his advice on EEG-video records, Bernard Secher and Rozenn Rougetet for providing computer software and hardware support, Brigitte Jouve and Floriane Fontaine for technical assistance and Richard Medeiros for his help in editing the manuscript. This work was supported by a grant from the Programme Hospitalier de Recherche Clinique, Assistance Publique - Hôpitaux de Paris (IDF94001).

REFERENCES

1. Willie E. Epilepsy surgery in infants. In: Willie E, ed. *The Treatment of Epilepsy: Principles and Practice*. Baltimore, MD: Williams and Wilkins; 1996:1087–1096.
2. Holmes MD, Dodrill CB, Ojemann LM, Ojemann GA. Five-year outcome after epilepsy surgery in nonmonitored and monitored surgical candidates. *Epilepsia*. 1996;37:748–752.
3. Spencer SS. The relative contribution of MRI, SPECT, and PET imaging in epilepsy. *Epilepsia*. 1994;35(suppl 6):S72–S89.
4. Devous MD, Thisted RA, Morgan GF, Leroy RF, Rowe CC. SPECT brain imaging in epilepsy: a meta-analysis. *J Nucl Med*. 1998;39:285–293.
5. Cross JH, Gordon I, Jackson GD, et al. Children with intractable focal epilepsy: ictal and interictal ^{99m}Tc HMPAO single photon emission computed tomography. *Develop Med Child Neurol*. 1995;37:673–681.
6. Harvey AS, Bowe AS, Hopkins IJ, et al. Ictal ^{99m}Tc-HMPAO single photon emission computed tomography in children with temporal lobe epilepsy. *Epilepsia*. 1993;34:869–877.
7. Harvey A, Hopkins I, Bowe J, Cook D, Shield L, Berkovic S. Frontal lobe epilepsy: clinical seizure characteristics and localization with ictal ^{99m}Tc-HMPAO SPECT. *Neurology*. 1993;43:1966–1980.
8. Menzel C, Steidele S, Grunwald F, et al. Evaluation of technetium-99m-ECD in childhood epilepsy. *J Nucl Med*. 1996;37:1106–1112.
9. Packard AB, Roach PJ, Davis RT, et al. Ictal and interictal technetium-99m-bicisate brain SPECT in children with refractory epilepsy. *J Nucl Med*. 1996;37:1101–1106.
10. Cross JH, Boyd SG, Gordon I, Harper A, Neville BG. Ictal cerebral perfusion related to EEG in drug resistant focal epilepsy of childhood. *J Neurol Neurosurg Psych*. 1997;62:377–384.
11. O'Brien TJ, So EL, Mullan BP, et al. Subtraction ictal SPECT co-registered to MRI improves clinical usefulness of SPECT in localizing the surgical seizure focus. *Neurology*. 1998;50:445–454.
12. Zubal IG, Spencer SS, Khursheed I, et al. Difference images calculated from ictal and interictal technetium-99m-HMPAO SPECT scans of epilepsy. *J Nucl Med*. 1995;36:684–689.
13. Véra P, De Dreuille O, Bendriem B, et al. Advantage of fan beam collimators for contrast recovery of hyperfixation in clinical SPECT. *IEEE Trans Nucl Med*. 1997;44:83–89.
14. Véra P, Farman-Ara B, Stiévenart JL, et al. Proportional anatomical stereotactic atlas for visual interpretation of brain SPECT perfusion images. *Eur J Nucl Med*. 1996;23:871–877.
15. Talairach J, Tournoux P. *Coplanar Stereotaxic Atlas of the Human Brain*. New York, NY: G. Thieme Verlag; 1988.
16. Mangin J, Frouin V, Bloch I, Bendriem B, Lopez-Krahe J. Fast-nonsupervised 3D registration of PET and MR images of the brain. *J Cereb Blood Flow Metab*. 1994;14:749–762.
17. Deriche R. Using Canny's criteria to derive a recursively implemented optimal edge detector. *Int J Comput Vision*. 1987;1:167–187.
18. Duncan R, Patterson J, Roberts R, Hadley DM, Bone I. Ictal/postictal SPECT in the presurgical localisation of complex partial seizures. *J Neurol Neurosurg Psych*. 1993;56:141–148.
19. Mauguière F, Ryvlin P. Morphological and functional neuro-imaging of surgical partial epilepsies in adults. *Rev Neurol*. 1996;152:501–516.
20. Duncan R, Rahi S, Bernard AM, et al. Ictal cerebral blood flow in seizures originating in the posterolateral cortex. *J Nucl Med*. 1996;37:1946–1961.
21. Ho SS, Berkovic SF, Newton MR, Austin MC, McKay WJ, Bladin PF. Parietal lobe epilepsy: clinical features and seizure localization by ictal SPECT. *Neurology*. 1994;44:2277–2284.
22. Laich E, Kuzniecki R, Mountz J, et al. Supplementary motor area epilepsy. Seizure localisation, cortical propagation and subcortical activation pathways using ictal SPECT. *Brain*. 1997;120:855–864.
23. Alfonso I, Harvey S, Acuna A, et al. Interictal and ictal SPECT in a neonate with hemimegaloencephaly. *Clin Nucl Med*. 1997;22:323–324.
24. Green C, Buchhalter JR. Ictal SPECT in a 16-day old infant. *Clin Nucl Med*. 1993;18:768–770.
25. Bye AM, Parle J, Haindl W. Single photon emission computed tomography in intractable infantile seizures. *Clin Exp Neurol*. 1993;30:117–123.
26. Kuzniecki R, Mountz JM, Wheatley G, Morawetz R. Ictal single-photon emission computed tomography localized epileptogenesis in cortical dysplasia. *Ann Neurol*. 1993;34:627–631.
27. Packard AB, Roach PJ, Davis RT, et al. Ictal and interictal technetium-99m-bicisate brain SPECT in children with refractory epilepsy. *J Nucl Med*. 1996;37:1101–1106.
28. Luna D, Dulac O, Plouin P. Ictal characteristics of cryptogenic partial epilepsy in infancy. *Epilepsia*. 1989;30:827–832.
29. Hertz-Pannier L, Gaillard WD, Mott SH, et al. Noninvasive assessment of language dominance in children and adolescents with functional MRI: a preliminary study. *Neurology*. 1997;48:1003–1012.
30. Véra P, Kaminska A, Cieuta C, et al. Localization of seizure foci in children using ictal and interictal SPECT scans co-registered to MRI [abstract]. *J Nucl Med*. 1997;38:12.
31. Newton MR, Berkovic SF, Austin MC, Rowe CC, McKay WJ, Bladin PF. SPECT localisation of extratemporal and temporal seizure foci. *J Neurol Neurosurg Psych*. 1995;59:26–30.